CrossMark

SCIENTIFIC ARTICLE

Higher fluorine-18 fluorodeoxyglucose positron emission tomography (FDG-PET) uptake in tuberculous compared to bacterial spondylodiscitis

Matteo Bassetti[1] · Maria Merelli[1] · Fernando Di Gregorio[2] · Paola Della Siega[1] ·
Maria Screm[3] · Claudio Scarparo[3] · Elda Righi[1]

Abstract

Background Tuberculous spondylodiscitis can be difficult to diagnose because of its nonspecific symptoms and the similarities with non-tubercular forms of spinal infection. Fluorine-18-fluorodeoxyglucose positron emission tomography combined with computed tomography (FDG PET-CT) is increasingly used for the diagnosis and monitoring of tubercular diseases.

Methods Retrospective, case-control study comparing tuberculous spondylodiscitis with biopsy-confirmed pyogenic spondylodiscitis in the period 2010–2012.

Results Ten cases of tuberculous spondylodiscitis and 20 controls were included. Compared to pyogenic, tuberculous spondylodiscitis was more frequent in younger patients ($P = 0.01$) and was more often associated with thoraco-lumbar tract lesions ($P = 0.01$) and multiple vertebral involvement ($P = 0.01$). Significantly higher maximum standardized uptake values (SUV) at FDG-PET were displayed by tuberculous spondylodiscitis compared to controls (12.4 vs. 7.3, $P = 0.003$). SUV levels above 8 showed the highest value of specificity (0.80). Mean SUV reduction of 48% was detected for tuberculous spondylodiscitis at 1-month follow-up.

Conclusions Higher SUV levels at FDG-PET were detected in tuberculous compared with pyogenic spondylodiscitis.

PET-CT use appeared useful in the disease follow-up after treatment initiation.

Introduction

Extra-pulmonary tuberculosis (TB) accounts for 15 to 20% of all TB cases [1]. Less than 1% of extra-pulmonary forms of TB involve the spinal tract, usually affecting the vertebral body or the posterior arch of the vertebra and the intervertebral disk, causing spondylodiscitis [1, 2]. Tuberculous spondylodiscitis (TBSD), also known as Pott's disease, is caused by hematogenous dissemination of the infection that can affect any segment of the spine [1–3]. In up to 40% of cases, the infection can disseminate to the adjacent vertebral bodies via longitudinal ligaments, causing complications such as plegia or paraparesis [1]. Clinical findings of TBSD include local tenderness, kyphotic deformity and, in severe forms, complete limitation of motion. Symptoms of TBSD, however, are usually nonspecific and characterized by a slow onset, contributing to delays in the diagnosis of the disease [1, 3]. TBSD diagnosis is usually based on the combination of symptoms, imaging and microbiological cultures; the gold standard, however, is represented by imaging-guided vertebral biopsy that allows discriminating between TBSD and pyogenic spondylodiscitis [1–3]. Magnetic resonance imaging (MRI), high-definition computed tomography (CT) and fluorine-18-deoxyglucose (FDG) positron emission tomography (PET) combined with CT (PET-CT) are used to describe the extension of the infectious process and may serve as a guide for biopsy [3, 4]. Recently, the use of FDG PET-CT

✉ Elda Righi
elda.righi@libero.it

1   Infectious Diseases Division, Santa Maria della Misericordia University Hospital, 50, Colugna Street, Udine 33100, Italy

2   Microbiology Unit, Santa Maria della Misericordia University Hospital, Udine, Italy

3   Radiology Unit, Santa Maria della Misericordia University Hospital, Udine, Italy

Springer

for the diagnosis of spondylodiscitis has increased. FDG, as a glucose analog, is taken up by high-glucose-using cells and is used in PET-CT because of its reduced metabolism, allowing FDG to be trapped in the cells [5]. FDG serves as a tracer for tumor detection since its accumulation via glucose transporters is based on enhanced glycolysis associated with the cell growth rate [6]. Inflamed or infected tissues, as well as chronic granulomatous diseases such as TB, can cause increased FDG uptake due to enhanced glucose metabolism, tissue permeability and the high number of glucose transporters [4].

Here we report a case-control study encompassing 10 cases of TBSD and 20 cases of pyogenic spondylodiscitis comparing clinical features and characteristics of FDG PET-CT.

Material and methods

Subjects

All cases of TBSD diagnosed over a 3-year period (2010–2012) were retrospectively included in the study and matched 1:2 to cases of biopsy-proven pyogenic spondylodiscitis (controls). All controls underwent FDG PET-CT.

Overall, 10 cases and 20 controls were analyzed. Definitions of non-tubercular spinal infection and of proven or probable TBSD were based on microbiological, clinical and histopathogical features as previously described [3]. In particular, proven TBSD was supported by the evidence of acid-fast bacilli (AFB) and/or caseous necrosis from specimens obtained from the affected site. The diagnosis of probable TBSD was based on suggestive TB features, including proven active tuberculosis in other body compartments (e.g., positive urine culture, positive sputum or positive stomach contents after fasting) in combination with clinical or radiological manifestations (X-ray, CT scan, MRI) that correlated with spinal tuberculosis and a good response to chemotherapy.

In all patients, CT or ultrasound-guided aspiration of paravertebral collections or pathological bone tissues was obtained according to our local protocol. The samples were analyzed for histological evidence of caseating granulomas along with microbiological evidence of AFB or other pathogens. Clinical follow-up was performed at 6 and 12 months after treatment.

The study was approved by the local institutional review board. All procedures performed were in accordance with the ethical standards of the institutional and national research committee and with the 1964 Helsinki Declaration and its later amendments or comparable ethical standards. Informed consent was waived because of the retrospective nature of the study.

Imaging

All lesions were analyzed using contrast-enhanced MRI and whole-body FDG PET-CT within 2 weeks from the onset of symptoms. Maximum standardized uptake value (SUV) of the most FDG avid lesions was recorded. In 8 out of 10 TBSD cases and in 14 out of 20 pyogenic spondylodiscitis cases, a repeated FDG PET-CT was performed after 1 month from the beginning of the treatment to detect a decrease in SUV.

PET-CT protocol

Scans were performed using a hybrid PET-CT scanner (Biograph 2; Siemens, Erlangen, Germany). Patients fasted for 4 to 6 h before intravenous injection of a dose of 5.5 Mbq/kg of FDG, and blood glucose levels were required to be less than 140 mg/dl. Up to 60 min was allowed for FDG uptake before PET-CT imaging acquisition. No intravenous contrast agent was administered for the CT part of the PET-CT scan. CT scan of the area between the proximal femora and base of the skull was acquired for attenuation correction of PET data and anatomic correlation. CT acquisition was performed with a spiral dual-slice CT scanner with 130 kV, 60 mAs, 5-mm slice thickness and a pitch of 1. Images were acquired using a matrix of 512×512 pixels and a pixel size of 1 mm. After CT acquisition, PET acquisition of the same axial range was completed and the patient kept in the same position. Three-dimensional PET acquisition required 2 to 3 min per bed position. PET data were acquired using a matrix of 128×128 pixels, and PET images were reconstructed using the iterative ordered subset expectation maximization method (four iterations and eight subsets) with a slice thickness of 5 mm. After completion of PET acquisition, the reconstructed attenuation-corrected PET images, CT images, and fused matched PET and CT images were available for review in the axial, coronal and sagittal planes, as well as maximum intensity projections (MIP), and in three-dimensional cine mode. Images were interpreted by a nuclear medicine specialist. The criterion for infection was visual, and a patient was considered positive when FDG uptake was higher than bone marrow uptake in adjacent vertebras and/or soft tissue uptake was present. In all patients, semiquantitative analysis was also performed using SUV. SUV was defined as the SUVmax in the region of interest (ROI) placed over the area surrounding the lesion suspected of infection and calculated from the following equation: (activity/unit volume)/(injected dose/total body weight).

Statistical analysis

Baseline characteristics were compared using a t test or one-way ANOVA for continuous variables and $\chi 2$ test for categorical variables. For variables that were not normally distributed,

the Mann-Whitney test was used. Variables including a P value < 0.05 were considered to be statistically significant. SUV cutoff values that correlated with tuberculous spondylodiscitis were calculated using Pearson's χ^2. The optimal cutoff point was determined through ROC curve analysis (e.g., maximum values of the Youden index calculated as SE + SP-1).

Results

Patients' characteristics and microbiological diagnosis

Overall, 10 cases of TBSD and 20 controls were detected during the 3-year study period. Among TBSD cases, five were proven and five were probable; of these, two cases had a proven TB diagnosis at a different site and three cases presented suggestive clinical and radiological features of TBSD. Patient demographic and clinical characteristics are reported in Table 1. Compared to controls, TBSD cases displayed younger mean age (P = 0.01) and were more often males (P = 0.01). Four (40%) patients with TBSD were from areas of high endemicity. Microbiological diagnosis was made through bone tissue culture in 9 (45%) patients and from percutaneous aspiration of paravertebral abscess in 11 (55%) cases of pyogenic spondylodiscitis. Among these, 13 (65%) had positive blood cultures.

MRI characteristics

A total of 27 (90%) patients underwent MRI to define the spinal lesions, while three patients could not have an MRI because of non-compatible devices. MRI characteristics showed a more frequent involvement of the thoraco-lumbar spinal tract among TBSD compared to pyogenic spondylodiscitis patients (60% vs. 10%, P = 0.01); furthermore, multiple intervertebral localizations of the disease were only detected among TBSD cases (two patients had 2, one had 5 and one had 8 intervertebral spaces involved, respectively), while all controls had only one intervertebral space involved. Muscular abscesses were found in 80% of cases (6 involving the psoas, 1 the para-spinosus and 1 the paravertebral muscles). Patients affected by TBSD were more likely to present focal, extra-osseous para-spinal masses compared to controls (80% vs. 35%, respectively, P not significant), especially in the area of the psoas. Among controls, muscular abscesses involved the paravertebral muscles in three cases, the gluteus muscles in two cases and the psoas or iliac muscles in two cases.

PET-CT features

Overall, no substantial discrepancies were detected between MRI and PET-CT regarding the localization of TB lesions.

Table 1 Demographic, clinical and radiological characteristics of tuberculous spondylodiscitis (TBSD) and pyogenic spondylodiscitis

Characteristics	TBSD (n = 10)	Pyogenic spondylodiscitis (n = 20)	P value
Mean age ± SD	45.3 ± 25.8	62.2 ± 9.9	0.01
N <40 years (%)	4 (40)	0	0.01
N >40 years (%)	6 (60)	20 (100)	0.01
Male sex (%)	9 (90)	6 (30)	0.01
Site of infection (%)			
Cervical-thoracic	0	0	NS
Thoracic	0	6 (30)	NS
Thoraco-lumbar	6 (60)	2 (10)	0.01
Lumbar	4 (40)	10 (50)	NS
Lumbar-sacral	0	2 (10)	NS
Sacral	0	0	NS
Multiple sites (%)	4 (40)	0	0.01
Extra-osseous masses (%)	8 (80)	7 (35)	NS
Psoas	6	1	NS
Paravertebral	1	3	NS
Paraspinosis	1	0	NS
Gluteus	0	2	NS
Iliac	0	1	NS
Median PET-CT SUV (range)	12.4 (6–22)	7.3 (4.1–13.4)	0.003

NS = not significant (P > 0.05)

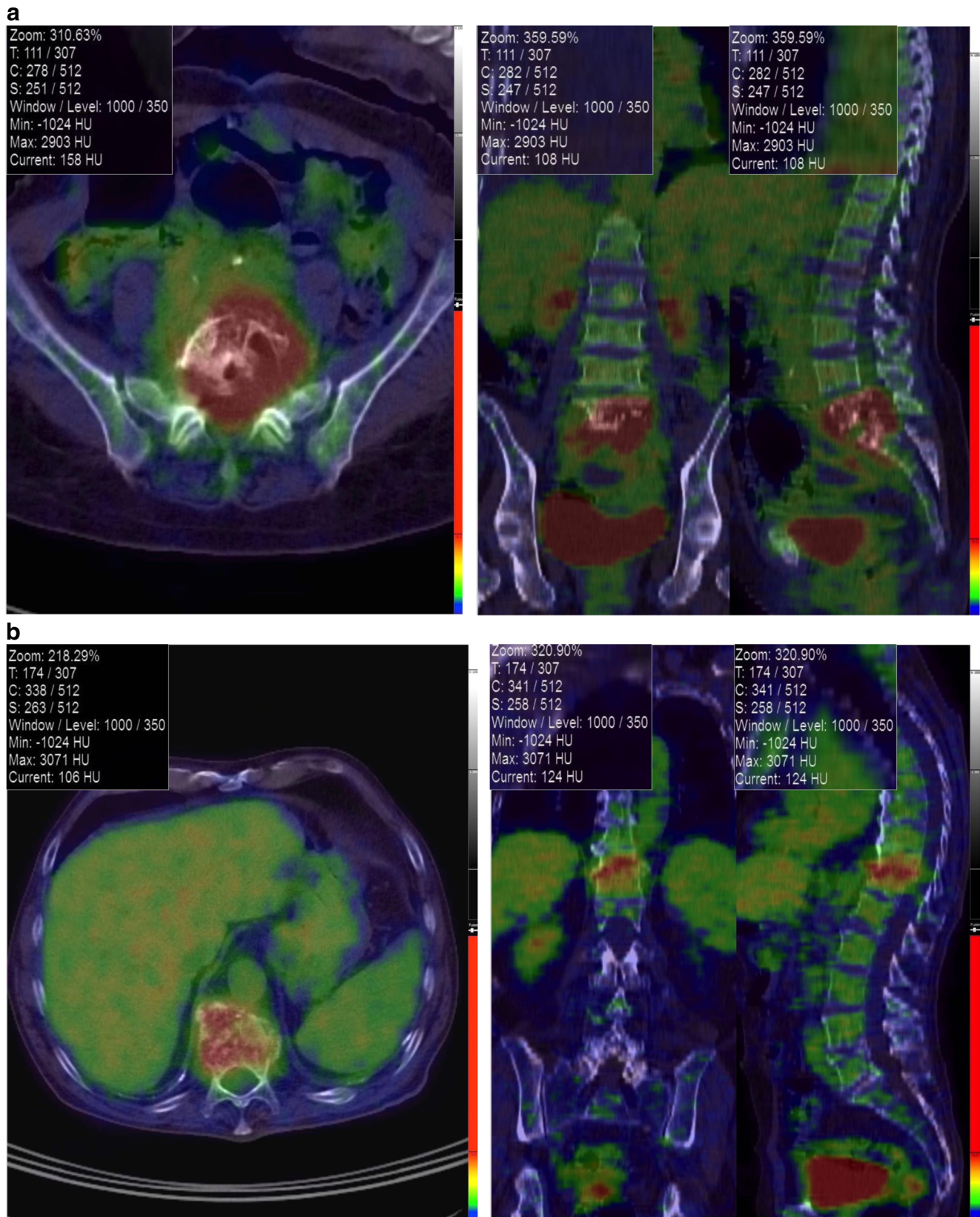SUV = standardized uptake value

Fig. 1 Representative transverse CT images and fused FDG-PET images of tuberculous (**a**) and pyogenic (**b**) spondylodiscitis. Tuberculous spondylodiscitis showed alterations between L4 and S1 extended to the ileo-psoas muscle (SUV 18.8). In pyogenic spondylodiscitis anomalies were limited to D12 with lower SUV (6.6)
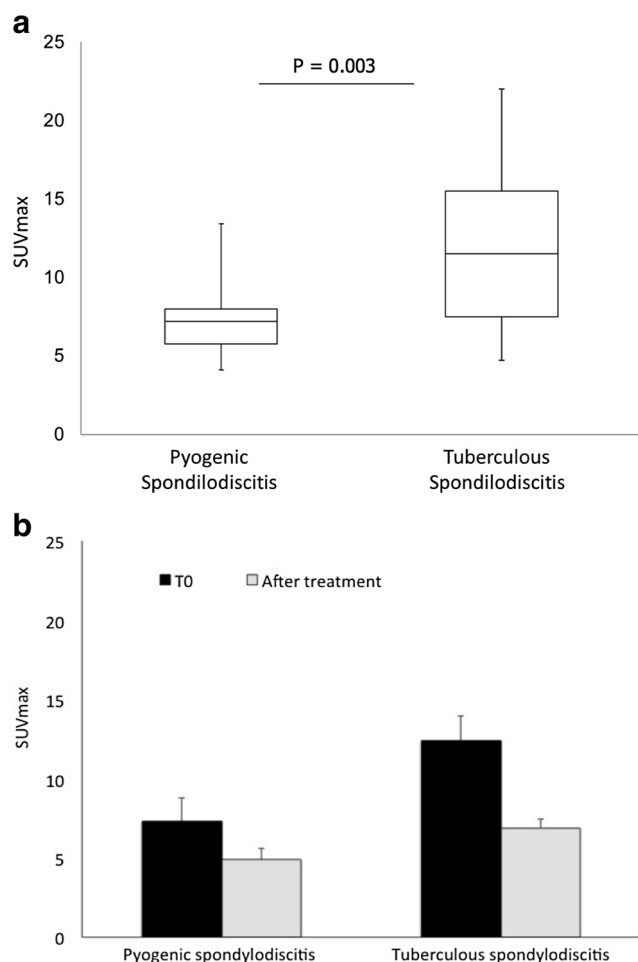
Fig. 2 **a** Comparison of maximum standardized uptake values (SUV) between pyogenic (n = 20) and tuberculous spondilodiscitis (n = 10); **b** reduction of SUV after treatment in pyogenic and tuberculous spondylodiscitis
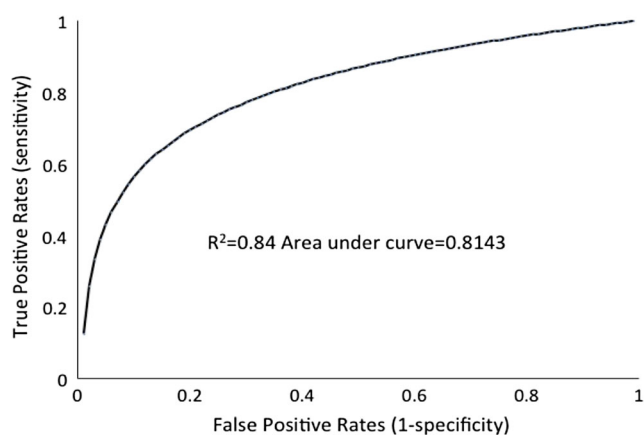

Fig. 3 Area under ROC curves for SUV >8 in the diagnosis of tuberculous spondylodiscitis

TBSD compared to pyogenic spondylodiscitis (P = 0.02) showing sensitivity of 0.80, specificity of 0.65, and maximum values of the Youden index. At a lower cutoff point, the specificity and positive predictive value were rather poor, although the sensitivity increased to 1.0. At a higher cutoff point, an increase in the specificity and positive predictive value was noted (from 0.65 to 0.85 and from 0.53 to 0.66, respectively), with a decrease in sensitivity to 0.60. The area under the ROC curve representing SUV at PET-CT is reported in Fig. 3.

Overall, all patients with TBSD and 11/14 (79%) with pyogenic spondylodiscitis displayed a reduction in the SUV value over time. A significant reduction of mean values (from 12.4 to 6.9, P = 0.02, and from 7.3 to 4.9, P = 0.06, respectively) was reported in both groups. Median reduction of SUV% was higher for TBSD compared to pyogenic spondylodiscitis although the difference was not significant (48% vs. 21%, P = 0.07) (Fig. 2b).

Patients' outcome

A total of five patients (17%) underwent surgical procedures (Table 3). Three patients, one from the TBSD group and two controls, had incision and drainage of muscle abscesses and removal of necrotic tissue. Two patients, one from the TBSD group and one control, presenting with neurological symptoms underwent laminectomy. All patients who had a surgical intervention displayed positive outcomes.

One patient from the TBSD group died after 4 months of treatment because of the development of lung cancer. Follow-up MRI was performed in 27 patients within 6 months from

FDG PET-CT characteristics showed significant differences between cases and controls (Fig. 1). Mean SUV value for TBSD was 12.4 (range, 6.0–22); two (20%) patients had an SUV between 6 and 8, two (20%) between 8 and 10, and six (60%) had SUV >10. Significantly lower SUV values were displayed by controls (7.3, range 4.1–13.4, P = 0.003, Fig. 2a). Among controls, eight (40%) had SUV <6, nine (45%) between 6 and 10, and three (15%) had SUV >10.

Table 2 summarizes the sensitivity, specificity, positive and negative predictive factor values for SUV in TBSD at significant cutoff points. SUV >8 significantly correlated with

	Values	Sensitivity	Specificity	Positive predictive value	Negative predictive value
Table 2 Sensitivity, specificity, positive predictive and negative predictive value of different SUV values at FDG-PET associated with tuberculous spondylodiscitis	SUV ≥6	1.0	0.40	0.45	1.0
	SUV ≥8	0.80	0.65	0.53	0.87
	SUV ≥10	0.60	0.85	0.66	0.81

Table 3 Type and outcome of surgical interventions among patients with tuberculous and pyogenic spondylodiscitis

Spondylodiscitis	Indication	Intervention	Outcome
Tuberculous	Large pluriconcamerate psoas abscess	Cavity debridement and drainage	Cured
Tuberculous	Rapid onset of paraparesis due to spinal cord compression (D11–D12), radicular compression and instability of L2–L3 vertebral bodies	Urgent D11–D12 laminectomy and endocanalar tissue removal; L3 laminectomy; partial L2 laminectomy, L1–L4 stabilization	Improved
Pyogenic	Gluteus muscle abscess	Incision and drainage	Cured
Pyogenic	Paravertebral purulent collection with contiguous pleural empyema	Drainage and left lung decortication	Cured
Pyogenic	Incomplete paraplegia	L2–L4 laminectomy and T10–L5 arthrodesis	Improved

the diagnosis, showing substantial improvement or stability of the infectious process in 89% and 11% of cases, respectively. At 12-month follow-up, all patients reported resolution of symptoms or clinical improvement.

Discussion

The differential diagnosis between TSBD disease and pyogenic spondylodiscitis can be challenging [1]. Delayed diagnosis of TBSD, furthermore, may lead to severe consequences, including permanent spinal damage [1, 2]. Although spinal biopsies often represent the most accurate diagnostic methods, low microbiological yields can be associated with TBSD; imaging therefore represents a key diagnostic tool to achieve early diagnosis of the disease and is often used to monitor the response to antibiotic treatment [1, 3]. Radiological characteristics often show that TBSD causes the involvement of several contiguous segments and is associated with para-spinal abscesses [1–3]. Our study confirmed TBSD typical involvement of the thoraco-lumbar spinal tract, presence of multiple intervertebral localizations and more frequent muscular abscesses compared with pyogenic spondylodiscitis using MRI and PET-CT. MRI follow-up after therapy, however, often shows minimal changes and may be difficult to interpret. FDG PET-CT is frequently used for the diagnostic workup of spinal localizations of infection as well as follow-up [4, 6–8]. Although high SUV values (e.g., greater than 2.5) are normally attributed to malignant lesions, the literature has reported elevated SUV values with peaks up to 21 in tuberculous lesions [6, 7].

In active pulmonary tuberculosis, the intense FDG uptake is attributed to a large number of activated macrophages presenting high glycolytic rates [9]. Specifically, the hexose monophosphate shunt is stimulated by phagocytosis, increasing up to 30 times compared to baseline values [10]. In chronic infectious processes, FDG accumulates in the marginal zone of young fibroblasts, in macrophages and also in the neutrophil layer and granulation tissue [9]. This could explain higher SUV values in spinal TB, which is often characterized by abscess formation and granulation tissue compared to other infectious lesions [11]. Other studies have reported that extrapulmonary TB can produce high radionuclide uptake in PET-CT and can detect both asymptomatic and abnormal lesions. Furthermore, in this context PET-CT showed encouraging results, particularly when MRI examination could not discriminate between degenerative changes and infection.

Non-tubercular bacterial infections at pulmonary or extrapulmonary sites can also present with increased SUV, posing a challenge in the differentiation with TB. A study analyzing the differences in SUV at PET-CT scans between tuberculous and non-tubercular mycobacterial infections in 26 patients showed results comparable to our study. In patients with pulmonary and lymphonodal tubercular disease, mean SUV was significantly higher (10.07 ± 6.45 and 7.23 ± 3.03, respectively) compared to non-tubercular mycobacterial lesions (3.59 ± 2.32 and 1.21 ± 0.29) [12].

Data have also suggested that FDG PET-CT can be used in monitoring the disease activity after treatment through the reduction of SUV in repeated imaging [13]. In a study encompassing 21 patients with TB, FDG PET-CT showed a median reduction of 31% in radiotracer uptake for 90% of patients [8]. Another report evaluating the role of sequential FDG PET-CT before and during treatment in 33 patients with skeletal TB showed mean SUV values of 15 (range 6 to 30) and a substantial decrease of uptake over time [4]. In our study, all patients showed a significant reduction of SUV over time.

To our knowledge, this is the first study comparing SUV between TBSD and pyogenic spondylodiscitis. Our report, however, is limited by its small size and by the retrospective nature. Nevertheless, we observed a significant difference between SUV in TBSD and control patients showing a cutoff value above 8 more often associated with TBSD disease compared to pyogenic spondylodiscitis. A limited sensitivity and the low number of subjects enrolled in the study, however, do not allow drawing definitive conclusions and warrant further studies in the area of PET-TC and spondylodiscitis.

Conclusions

Overall, our report supports the use of FDG PET-CT in the management of TBSD, especially in the follow-up of the

disease after therapy. In particular, PET-CT can be used in association with MRI for the detection of the disease, but can also contribute to the early determination of the response to therapy. The association of specific PET-CT features, such as high SUV, with TBSD has been previously reported but remains to be determined. Large, prospective studies analyzing the use of PET-CT in TBSD and in other infectious forms of spondylodiscitis, such as pyogenic spondylodiscitis, are encouraged to improve the management of this disease.

References

1. Trecarichi EM, Di Meco E, Mazzotta V, Fantoni M. Tuberculous spondylodiscitis: epidemiology, clinical features, treatment, and outcome. Eur Rev Med Pharmacol Sci. 2012;16 Suppl 2:58–72.

2. Rasouli MR, Mirkoohi M, Vaccaro AR, Yarandi KK, Rahimi-Movaghar V. Spinal tuberculosis: diagnosis and management. Asian Spine J. 2012;6(4):294–308.

3. Mirsaeidi SM, Tabarsi P, Amiri MV, et al. Clinical and radiological presentation of adult tuberculous spondylitis. Tanaffos. 2003;2(6): 59–65.

4. Dureja S, Sen IB, Acharya S. Potential role of F18 FDG PET-CT as an imaging biomarker for the noninvasive evaluation in uncomplicated skeletal tuberculosis: a prospective clinical observational study. Eur Spine J. 2014;23(11):2449–54.

5. Mochizuki T, Tsukamoto E, Kuge Y, Kanegae K, Zhao S, Hikosaka K, et al. FDG uptake and glucose transporter subtype expressions in experimental tumor and inflammation models. J Nucl Med. 2001;42:1551–5.

6. Yang CM, Hsu CH, Lee CM, Wang FC. Intense uptake of [F-18]-fluoro-2 deoxy-D-glucose in active pulmonary tuberculosis. Ann Nucl Med. 2003;17:407–10.

7. Heysell SK, Thomas TA, Sifri CD, Rehm PK, Houpt ER. 18-fluorodeoxyglucose positron emission tomography for tuberculosis diagnosis and management: a case series. BMC Pulm Med. 2013;13:14.

8. Martinez V, Castilla-Lievre MA, Guillet-Caruba C, et al. (18)F-FDG PET-CT in tuberculosis: an early non-invasive marker of therapeutic response. Int J Tuberc Lung Dis. 2012;16(9):1180–5.

9. Kubota R, Yamada S, Kubota K, Ishiwata K, Tamahashi N, Ido T. Intratumoral distribution of fluorine-18-fluorodeoxyglucose in vivo: high accumulation in macrophages and granulation tissues studied by microautoradiography. J Nucl Med. 1992;33:1972–80.

10. Amerein PC, Larson SM, Wagner Jr HN. An automated system for measurement of leukocyte metabolism. J Nucl Med. 1975;15:352–5.

11. Bakheet SM, Powe J, Ezzat A, Rostom A. F-18-FDG uptake in tuberculosis. Clin Nucl Med. 1998;23:739–42.

12. Del Giudice G, Bianco A, Cennamo A, Santoro G, Bifulco M, Marzo C, et al. Lung and nodal involvement in nontuberculous mycobacterial disease: PET/CT role. Biomed Res Int. 2015;2015: 353202.

13. Razak A, Rahim NA, Nordin AJ. Dual time point imaging of FDG PET/CT in a tuberculous spondylodiscitis. Biomed Imag Interv. 2010;6(2):e18.